Chapter 7
Summary and future prospects

The research in this thesis is focused on delineating the stereoelectronic effects exerted by ring substituents on carbohydrate derived oxocarbenium, iminium and ammonium ions. The electronegative oxygen substituents on the carbohydrate rings have an intrinsic (inductive) destabilizing effect on the positive charge of these cations. The magnitude of the destabilization depends on the nature of the substituent, its position and orientation on the carbohydrate ring. For example, it has long been known that axially positioned alkoxy groups at the C4 of pyranosides are less destabilizing than their equatorially

oriented counterparts. This becomes apparent in the higher reactivity of galactosyl donors in comparison to identically functionalized glucosyl donors and the faster hydrolysis of nitrophenol galactosides with respect to their glucosyl congeners. This reactivity difference can be explained by the stabilization of the electron depleted anomeric center by through space electron density donation of the axially positioned oxygen substituent. In addition, the interaction of the C4-O dipole with the positive charge at the anomeric center is more favorable in the galactose case than in the glucose case. To allow for the most optimal stabilization or to diminish the destabilizing effect of the substituents, carbohydrates can change their conformation to optimally position the ring substituents. The conformation of the carbohydrate ring can be a decisive factor in determining the stereochemical course of an addition reaction to the anomeric center. Similarly, protonation of iminosugars can change their conformation, thereby influencing the affinity of the molecule for the active site of its enzyme target.

In **Chapter 1** a general introduction is given on stereoelectronic effects and how they guide conformational preferences. The stereoelectronic effects of individual substituents in furanoses and pyranoses is summarized, as well as the stereoelectronic effects that are at play in polyhydroxylated iminosugars.

Chapter 2 describes a study toward substitution reactions of the four possible D-pentofuranosyl (*i.e.* ribosyl, arabinosyl, xylosyl and lyxosyl) acetates with [D]triethylsilane. It was observed that all furanosides gave the 1,2-*cis* products with good to excellent stereoselectivity. This striking result was explained using the conformational preferences of the intermediate oxocarbenium ions, which were assessed by calculating free energy surface (FES) maps of the complete conformational space for these molecules. Using the "inside attack model" the results from the [D]triethylsilane substitution reactions could be correlated to the most stable oxocarbenium ion conformers found with the FES. The results corroborated previous findings that a C2 alkoxy group prefers a pseudoequatorial position for optimal stabilization of the oxocarbenium ion, while the C3 alkoxy group prefers to be positioned pseudoaxial. In contrast to previous results, the C4 methyleneoxyalkyl substituent proved to be of great importance. The C5-oxygen can take up a *gg*, *tg*, *gt* orientation with respect to the C4 atom and the different rotamers have distinctly different FES maps. Most stabilization can be provided by the *gg*-C5-oxygen if the C4 substituent is positioned in an axial fashion to allow for optimal through-space interactions. Also the interplay between the different substituents became apparent from the different FES maps. The methodology of Chapter 2 was extended to anomeric tertiary oxocarbenium ions in **Chapter 3**. Reduction of furanosyl ketoses with triethylsilane provides access to (naturally occurring) *C*-glycosides and it was shown that addition of the hydride to the ketoses occurred preferentially in a 1,2-*cis* manner. While an alkyl

substituent on the anomeric carbon did not change the stereoselectivity in the [D]TES addition reactions when compared to the analogous reaction with the aldoses as described in Chapter 2, a phenyl substituent did give some erosion of stereoselectivity in two out of four cases. Also in this case, the calculated FES could be used to account for the (diminished) stereoselectivity of the reactions. There was a slight difference in stereochemical outcome found in the experiments and those determined from the calculated oxocarbenium ion conformer preferences. The secondary cations described in Chapter 2 are less stable than the ketose oxocarbenium ions of Chapter 3 and therefore the structures in the transition states of the addition reactions will more closely resemble the oxocarbenium ion structure in the aldose case than in the ketose case. In other words: the transition state in the aldose case will be earlier. In the ketose case the transition state will also be more crowded because of the tertiary nature of the cations. Thus, the differences in ground state energy of the oxocarbenium ion conformers are a better predictor for the product ratio found in the reactions of the aldoses than for those seen with the ketoses.

The methodology used in Chapter 2 and 3 can be expanded to all kinds of five-membered rings to examine their stability and conformational preferences. It can provide an attractive means to investigate the influence of ring substituents on oxocarbenium ion intermediates. Relevant examples of groups that are commonly employed in oligosaccharide and natural product synthesis include azides, amides and carbamates employed to mask amino groups,[1] esters and carbonates used to protect alcohol groups,[1] fluorides that are often used as a mimic for hydroxyl groups and as stabilizing groups for anomeric linkages,[2-3] and carboxylates esters as present in masked glycuronic acids.[4-6] To dissect the electronic and steric effects of the C4 methyleneoxy group, it would be of interest to investigate the C4 propyl analogues. Figure 7.1 depicts the FES maps calculated for a set of arabinosyl oxocarbenium ions featuring a C2-azide, a C2-fluoride, a C4-carboxylate or a C4-propyl group. The FES map for the protected 2-azido arabinofuranose oxocarbenium ion (**1**) in Figure 7.1 shows that **1** has a broader conformational preference than its C2-OMe analogue (See Chapter 2). The preference for the all-equatorial oxocarbenium ion has decreased and the favorable conformers now also include the flat- and E_3 envelope with a small ring pucker. The C4-C5 *gg* rotamer provides the most stable oxocarbenium ion conformers in line with the C2-OMe arabinosyl ion. It is likely that the broader conformation preference will result in addition reactions that proceed with less selectivity, but this has to be established experimentally.

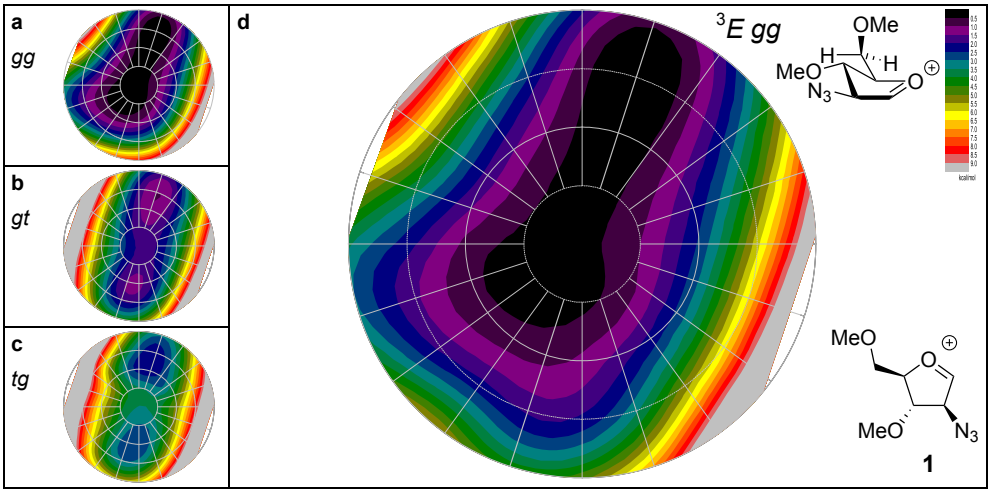

Figure 7.1 FES map of the 2-azidoarabinofuranosyl oxocarbenium ion (**1**). a) FES of the *gg* conformer. b) FES of the *gt* conformer. c) FES of the *tg* conformer. d) Global minimal FES of **1** showing the lowest-energy ^{3}E (*gg*) conformer.

The 2-fluoro arabinofuranosyl oxocarbenium ion FES map (**2**, Figure 7.2) more closely resembles that of the C2-OMe arabinosyl ion. However, the E_3 conformer now is not as unfavorable. This is likely the result of the smaller size of the C2 fluorine leading to a decrease in steric interaction between the C2 and C4 substituents in the E_3 envelope.

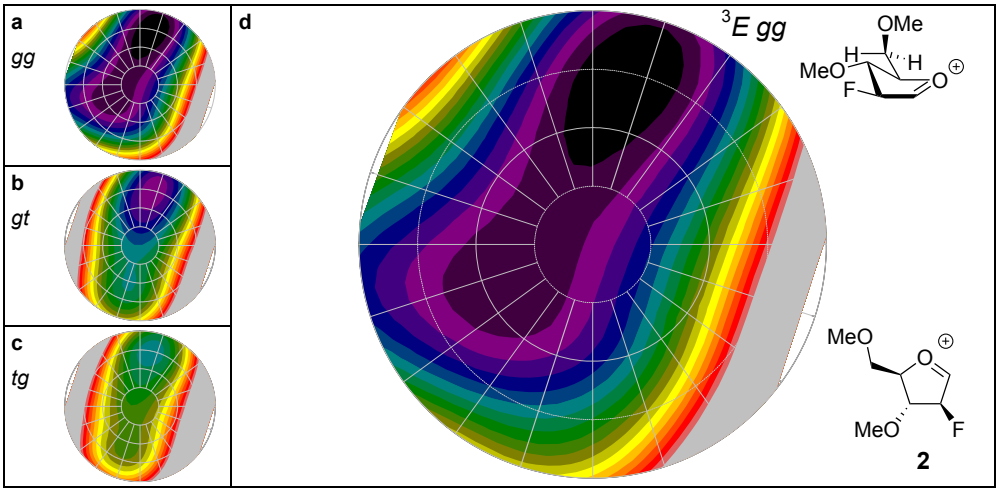

Figure 7.2 FES map of the 2-fluoroarabinofuranosyl oxocarbenium ion (**2**). a) FES of the *gg* conformer. b) FES of the *gt* conformer. c) FES of the *tg* conformer. d) Global minimal FES of **2** showing the lowest-energy ^{3}E (*gg*) conformer.

The effect of a C4 carboxylic ester on the relative stability of the oxocarbenium ion conformers is visualized in Figure 7.3a-c using arabinosyl oxocarbenium ion **3**. In contrast to the three staggered rotamers that the methyleneoxymethyl group can adopt, the

methyl ester can be found in two relatively favorable positions: *syn*, with the carbonyl pointing towards O4 and *anti*, with the carbonyl opposite O4 (Figure 7.3d). The calculations of the individual *syn*- and *anti*-conformers show that there is only a very small difference between the *anti* and *syn* conformers. Notably, the FES map now shows two local minima one on the side of the ^3E envelope and one on the opposite side of the E_3 envelope. In line with the findings described for the mannuronic acid oxocarbenium ions, (see Chapter 1 and 6) the stability of the E_3 envelope (which was unfavorable for the "non-oxidized" arabinosyl oxocarbenium ion, see Chapter 2) can result from extra stabilization by the axial C4 carboxylic ester[4] and the smaller steric requirements for this group.

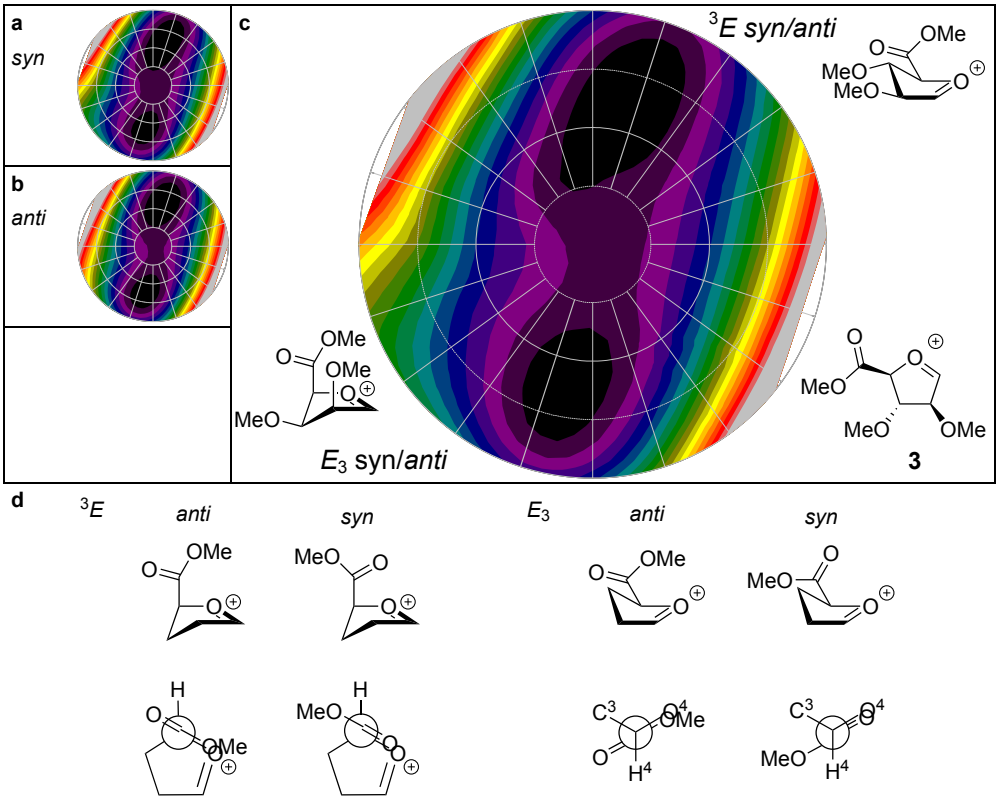

Figure 7.3 FES map of the C4 carboxylic ester arabinofuranosyl oxocarbenium ion (**3**). a) FES of the *syn* conformer. b) FES of the *anti* conformer. c) Global minimal FES of **3**. d) Possible rotamers around C4-C5 for the C5 carboxylate.

When O5 is replaced by a methylene group as in arabinose analogue **4**, the *gg* rotamer is no longer the most favorable rotamer (Figure 7.4). Instead the 'electronically neutral' alkyl prefers a *gt*-orientation for steric reasons. The FES map of arabinose **4** shows two local energy minima, an absolute minimum on the side of the ^3E conformation and a minimum (+0.9 kcal mol^{-1}) for the E_3 conformer.

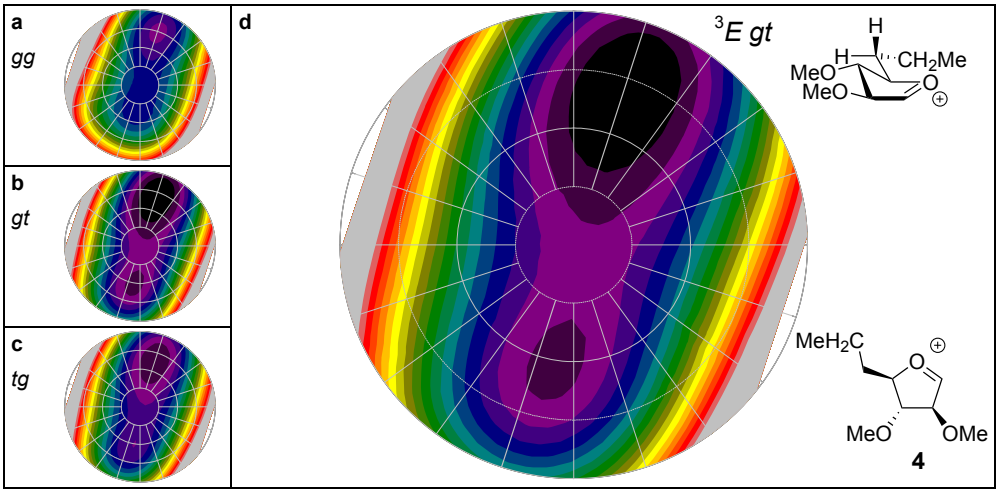

Figure 7.4 FES map of the 5-deoxy-5-ethyl arabinofuranosyl oxocarbenium ion (**4**). a) FES of the *gg* conformer. b) FES of the *gt* conformer. c) FES of the *tg* conformer. d) Global minimal FES of **4** showing the lowest-energy ^{3}E (*gt*) conformer.

It will be of interest to also map the FES of the *ribo*-, *xylo*-, and *lyxo*-configured oxocarbenium ions to deliver a detailed picture on the influence of the different functional groups. Similarly all the "stripped" analogues, featuring a single substituent, will provide information on the effect of the isolated substituent. The theoretical studies should be complemented by experiments to validate the outcome of the studies. This will provide an in-depth understanding of the stereoelectronic effects of the ring substituents, both in a stand-alone situation and in concert with other ring substituents.

In **Chapter 4**, a combination of experiments and calculations is described to investigate the conformation of carbohydrate derived iminium ions as well as the stereochemical course of the Ugi multicomponent reaction. To this end, the four possible D-pentofuranosyl imines were generated and reacted with a carboxylic acid and an isocyanide. The results indicated that the stereoselectivity of the Ugi reaction is determined in the addition step of the isocyanide to the iminium ion. It was therefore concluded that the studied reactions proceeded under kinetic control, in contrast to common conception that the Ugi reaction proceeds under thermodynamic control. The calculations show that after formation of the nitrilium adduct an exothermic and irreversible step provides the imidate, which then rearranges into the product in another exothermic reaction. It was also found that an axial C3-alkoxy substituent plays a role in the transition state of the cyanide addition step as it stabilizes the developing positive charge on the forming iminium ion. It would therefore be interesting to investigate the Ugi reaction using differentially substituted imines, for example those devoid of a substituent at C3 or imines featuring azides or fluorides in analogy to the studies described above.

Chapter 5 describes the generation of an extensive library of lipophilic furanosyl iminosugars. To this extent, a highly efficient synthesis route was used to generate all eight D- and L-iminofuranoses employing a double displacement cyclization delivering the amines in 6-7 steps from the unprotected pentoses. The eight stereoisomers were alkylated with seven different alkyl groups to furnish a library consisting of 64 compounds. The compounds can be subjected to enzyme inhibition assays to determine their activity in the search for novel glycolipid-processing enzyme inhibitors.[7]

The conformation of the furanosyl iminosugars of Chapter 5 can be analyzed using the FES mapping method developed in this Thesis. Protonation of the endocyclic nitrogen can lead to important structural changes as outlined before. As an initial example both the non-protonated and protonated *N*-methylated arabinose iminosugar were investigated (Figure 7.5). The non-protonated iminosugar preferably takes up a conformation around the ^{0}E envelope where all its substituents are in a sterically favored pseudoequatorial position. In the protonated ammonium ion, the preference shifts towards the E_1, a conformer with more pseudoaxial substituents. This shift can be explained to result from the stereoelectronic effects that develop upon protonation of the endocyclic amine. In contrast to the C4-C5 *gg*-rotamer that the unprotonated amine adopts, the protonated iminosugar preferentially adopts a C4-C5 *gt*-conformation because of an increased C2-C4 steric repulsion. The arabinosyl iminosugar **7** was analyzed by ^{1}H NMR and its conformation was identified by a mathematical approach.[8-9] It was determined that the arabinosyl iminosugar takes up an E_1 envelope structure, in line with the results of the FES map.

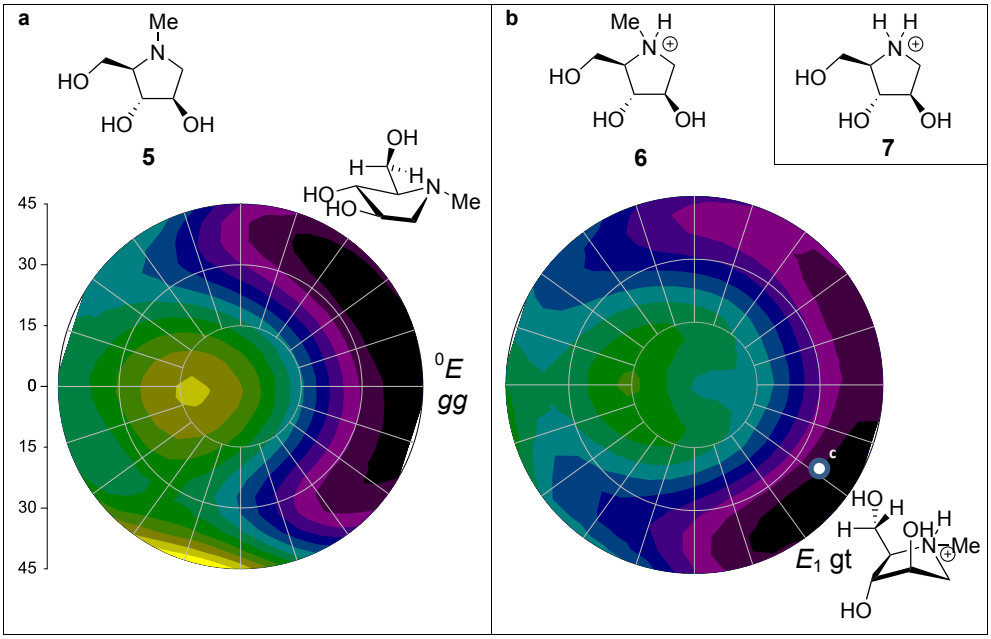

Figure 7.5 a) Global FES map of N-methyl arabinose iminosugar **5**. b) Global FES map of protonated N-methyl arabinose iminosugar **6**. c) Conformation identified from ^{1}H NMR for protonated arabinosyl iminosugar **7** (P: 122°, τ_m: 36).

Furanosyl iminosugars are known to not only target furanose processing enzymes but also inhibit pyranosidases.[10] The smaller size of the five membered ring iminosugars allows them to fit into the active site of pyranose processing enzymes. The substituent configuration plays an important role in the selectivity of inhibitors. Arabinosyl iminosugar **8** for example is a good inhibitor of both glucosidases and mannosidases. This inhibitory activity can be explained by comparing the optimal ^0E arabinosyl iminosugar conformation with D-glucose (**10**) and D-mannose (**11**), residing both in a $^4C_1$ chair conformation (Figure 7.6). The C2-C4 furanosyl substituents can be aligned with C3-C5 pyranosyl substituents, indicating that the substitution pattern of the 1,4-imino arabinitol allows for proper interactions with the active site (**9**).[11] However it should be noted that protonation of the amino groups can lead to a major conformational change and it remains to be seen how this influences the potency and selectivity of the furanosyl inhibitors. Studying the conformational preferences of both the protonated and non-protonated furanosyl (and pyranosyl) iminosugars will provide detailed insight to account for observed structure-activity-relationships.

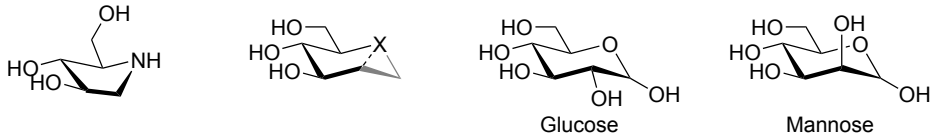

8 **9** **10** **11**

Figure 7.6 Structure of glucosyl and mannosyl inhibitor **8** aligned as in **9** with $^4C_1$ D-glucose (**10**) or D-mannose (**11**).

The conformational flexibility displayed by mannuronic acid iminosugars upon protonation is described in **Chapter 6**. Mannuronic acid donors show remarkable 1,2-*cis*-stereoselectivity and reactivity in glycosylation reactions. It has been proposed that the mannuronic acid $^3H_4$ oxocarbenium is at the basis of the striking reactivity. In this oxocarbenium ion all ring substituents are optimally positioned to stabilize the electron depleted anomeric center.[12] In Chapter 6 the conformational behavior of a set of mannuronic acid derived iminosugars was studied by NMR spectroscopy and through DFT calculations. It was found that the conformational flexibility displayed by mannuronic acid glycosyl donors extends to mannuronic acid iminosugars. Deoxymannojirimycin (DMJ) and three C6-oxidized analogues (the acid, the methyl ester and the amide) were studied. DMJ and the amide did not show any conformational change upon protonation, while both the acid and methyl ester gave a mixture of the $^4C_1$ and $^1C_4$ chair conformers. In D_2O the methyl ester gave a 56:44 mixture of the two chairs while in MeOD, a more apolar solvent in which the stereoelectronic stabilizing effects are more pronounced, the preference of the methyl ester for the "ring-flipped" $^1C_4$ chair was even stronger, and the molecule was found to adopt solely this conformation. The amide did not change conformation and the calculations revealed that the more stable $^4C_1$ conformation is caused by a hydrogen bond between the amide NH and O4. This molecule may be more prone to undergo a conformational change if this hydrogen bond can not form. Dimethylamide **12** is therefore an interesting iminosugar to investigate. Other C-5 substituents that are worthwhile to probe for their effect on the conformational equilibrium are the ketone **13** and CF_3-ketone **14**.

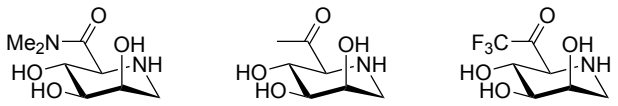

12 **13** **14**

Figure 7.7 C5 analogues for mannuronic acid iminosugars interesting to investigate their conformational preferences.

The conformational flexibility of the mannuronic acid iminosugars may be used to generate selective enzyme inhibitors. For example, the cleavage of mannosyl residues by

mannosidases belonging to glycosyl hydrolase family 47 (GH47) occurs through a pathway in which the mannosyl substrate follows a $^{3}S_{1} \rightarrow {}^{3}H_{4}^{\ddagger} \rightarrow {}^{1}C_{4}$ itinerary. The known mannosidase inhibitor mannoimidazole (**15**) effectively mimics the transition state by adopting a $^{3}H_{4}$ half-chair conformation (**16**). Under acidic conditions the mannuronic acid based iminosugars preferentially adopt a $^{1}C_{4}$ chair (**18**) that is conformationally close to the $^{3}H_{4}$ transition state and they may therefore be well suited as transition state mimics.

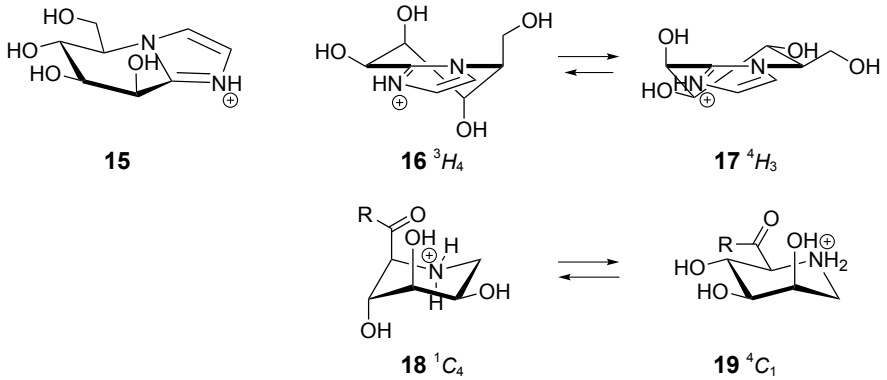

15 **16** $^{3}H_{4}$ **17** $^{4}H_{3}$

18 $^{1}C_{4}$ **19** $^{4}C_{1}$

Figure 7.8 Mannosyl inhibitor mannoimidazole **15** adopts a $^{3}H_{4}$ half-chair, mannuronic acid based iminosugars (**18**/**19**) adopt a conformationally close $^{1}C_{4}$ chair.

References

[1] Demchenko, A. V.*, Handbook of Chemical Glycosylation*, **2008**.

[2] Williams, S. J.; Withers, S. G. *Carbohydr. Res.* **2000**, *327*, 27-46, 10.1016/s0008-6215(00)00041-0.

[3] Walvoort, M. T. C.; Kallemeijn, W. W.; Willems, L. I.; Witte, M. D.; Aerts, J. M. F. G.; van der Marel, G. A.; Codée, J. D. C.; Overkleeft, H. S. *ChemComm* **2012**, *48*, 10386-10388, 10.1039/c2cc35653h.

[4] Dinkelaar, J.; de Jong, A. R.; van Meer, R.; Somers, M.; Lodder, G.; Overkleeft, H. S.; Codée, J. D. C.; van der Marel, G. A. *J. Org. Chem.* **2009**, *74*, 4982-4991, 10.1021/jo900662v.

[5] Walvoort, M. T. C.; Lodder, G.; Overkleeft, H. S.; Codée, J. D. C.; van der Marel, G. A. *J. Org. Chem.* **2010**, *75*, 7990-8002, 10.1021/jo101779v.

[6] de Jong, A. R.; Hagen, B.; van der Ark, V.; Overkleeft, H. S.; Codée, J. D. C.; van der Marel, G. A. *J. Org. Chem.* **2012**, *77*, 108-125, 10.1021/jo201586r.

[7] Ghisaidoobe, A.; Bikker, P.; de Bruijn, A. C. J.; Godschalk, F. D.; Rogaar, E.; Guijt, M. C.; Hagens, P.; Halma, J. M.; van't Hart, S. M.; Luitjens, S. B.; van Rixel, V. H. S.; Wijzenbroek, M.; Zweegers, T.; Donker-Koopman, W. E.; Strijland, A.; Boot, R.; van der Marel, G.;

Overkleeft, H. S.; Aerts, J. M. F. G.; van den Berg, R. J. B. H. N. *ACS Med. Chem. Lett.* **2011**, *2*, 119-123, 10.1021/ml100192b.

[8] Deleeuw, F.; Altona, C. *J. Comput. Chem.* **1983**, *4*, 428-437, 10.1002/jcc.540040319.

[9] Hendrickx, P. M. S.; Martins, J. C. *Chem Cent J* **2008**, *2*, 10.1186/1752-153x-2-20.

[10] Fleet, G. W. J.; Nicholas, S. J.; Smith, P. W.; Evans, S. V.; Fellows, L. E.; Nash, R. J. *Tetrahedron Lett.* **1985**, *26*, 3127-3130, 10.1016/s0040-4039(00)98636-2.

[11] Saotome, C.; Wong, C. H.; Kanie, O. *Chem. Biol.* **2001**, *8*, 1061-1070, 10.1016/s1074-5521(01)00074-6.

[12] Walvoort, M. T. C.; Dinkelaar, J.; van den Bos, L. J.; Lodder, G.; Overkleeft, H. S.; Codée, J. D. C.; van der Marel, G. A. *Carbohydr. Res.* **2010**, *345*, 1252-1263, 10.1016/j.carres.2010.02.027.